Electron-capture cross sections for low-energy highly charged neon and argon ions from molecular and atomic hydrogen

Cüneyt Can, Tom J. Gray, S. L. Varghese,* J. M. Hall, and L. N. Tunnell

James R. Macdonald Laboratory, Department of Physics, Kansas State University, Manhattan, Kansas 66506

(Received 6 July 1984)

Electron-capture cross sections for low-velocity (10^6-10^7 cm/s) highly charged Ne^{q+} ($2 \leq q \leq 7$) and Ar^{q+} ($2 \leq q \leq 10$) projectiles incident on molecular- and atomic-hydrogen targets have been measured. A recoil-ion source that used the collisions of fast heavy ions (1 MeV/amu) with target gas atoms was utilized to produce slow highly charged ions. Atomic hydrogen was produced by dissociating hydrogen molecules in a high-temperature oven. Measurements and analysis of the data for molecular- and atomic-hydrogen targets are discussed in detail. The measured absolute cross sections are compared with published data and predictions of theoretical models.

I. INTRODUCTION

Recently there has been increased interest in the study of electron capture by low-energy highly charged (LEHQ) ions from atoms and molecules. The reasons for this active research range from the study of the basic physics of such collisions to their recognized role in high-temperature plasma applications such as tokamaks. Electron capture by highly charged impurity ions in a plasma is most likely to proceed into high-lying excited states of the ion. The resulting line radiation is known to be a major source of energy loss for the plasma.[1] The efficiency of neutral-beam heating of a plasma may also be affected due to electron capture by the impurity ions from the injected neutral atoms.[2]

Electron capture from molecular and atomic hydrogen is of a special interest for several reasons. Since isotope effects are negligible, a systematic study of electron capture by highly charged ions at keV energies, particularly from hydrogen atoms, is necessary for current fusion studies and for fast-neutral-beam injection systems involving hydrogen or deuterium.

The experimental investigation of electron capture from molecular and atomic hydrogen is being actively pursued by several laboratories. Until recently the experimental work has been somewhat limited due to the difficulty in producing LEHQ heavy ion beams. Measured cross sections for partially ionized projectiles of a wide range of atomic numbers incident on molecular and atomic hydrogen have been reported.[3] Recent progress in experimental techniques has made it possible to study electron-capture collisions of highly charged or bare projectiles with hydrogen atoms at low collision velocities.[4]

We have measured absolute electron-capture cross sections for low-velocity (10^6-10^7 cm/s) Ne^{q+} ($2 \leq q \leq 7$) and Ar^{q+} ($2 \leq q \leq 10$) projectiles incident on molecular and atomic hydrogen. The experimental techniques of these measurements and the data normalization that was used to obtain absolute cross sections for atomic hydrogen are presented in Sec. II. The results of this work are discussed and compared in Sec. III with the predictions of the theoretical models and the published data from the experiments carried out by Huber[5] and Seim *et al.*[6] for $Ne^{q+}+H_2$ and $Ne^{q+}+H$ and by Huber,[5] Crandall *et al.*,[7] and unpublished data[8] for $Ar^{q+}+H_2$ and $Ar^{q+}+H$.

II. EXPERIMENT

The measurements of electron-capture cross sections for LEHQ ions from hydrogen is described in two separate sections for molecular- and atomic-hydrogen targets, respectively. Although these measurements share similar experimental techniques and can be considered interdependent, one observes increasing difficulty in the case of the atomic-hydrogen target. The relationship between the two types of measurements and the normalization procedure used in this work to obtain absolute cross sections for electron capture from the hydrogen atom are also presented in this section.

A. Electron capture from molecular hydrogen

The LEHQ ions used in these experiments were produced by the recoil-ion technique. More detailed discussion of the source and the physics of the collision between the fast heavy ion and the target atom are given elsewhere.[9-12] The ions produced in this way can be extracted out of the source with predetermined energies and used as a secondary beam for ion-atom collision studies at low velocities as was shown initially by Cocke *et al.*[9] and Justiniano *et al.*[13]

The experimental work of this paper was performed at Kansas State University using the James R. Macdonald laboratory 6-MV EN tandem Van de Graaff accelerator. The measurements of the electron-capture cross sections by LEHQ ions from the H_2 target was carried out using the experimental setup (Fig. 1) that has been described previously.[14] Therefore only a brief description of the measurements will be presented here.

In this experiment a pulsed 19-MeV F^{4+} (in some cases post-stripped to F^{8+}) beam from the accelerator was passed through a gas target at a pressure of 0.4 mTorr. The recoil ions were extracted out of the interaction region by an electric field applied at right angles to the pri-
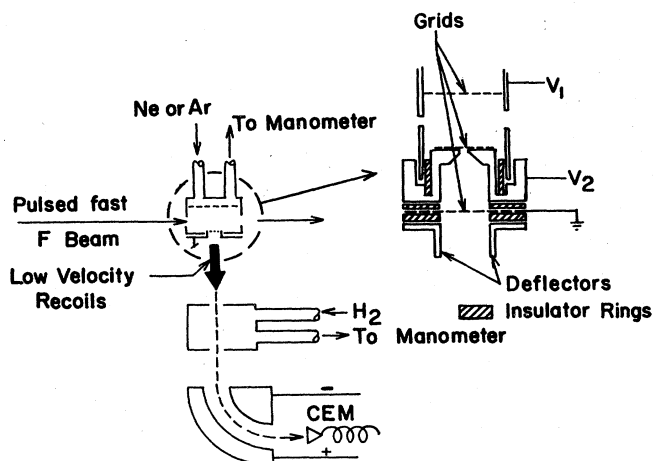
FIG. 1. Experimental arrangement for the recoil-ion source employed for the H_2 results in this work. Accelerating voltages V_1 and V_2 ($V_1 > V_2 > 0$) are applied to insulated electrodes as shown in the insert.

FIG. 3. Voltage sweep spectrum showing analog output containing charge exchange events labeled as $q - q'$, where q is the initial recoil-ion charge state and q' is the detected charge state.

mary beam and directed through a 1.68-cm-long gas cell containing molecular hydrogen. The entrance and exit apertures of this cell were 1 and 2.5 mm in diameter, respectively. The gas pressure in the cell (0.4 mTorr) was measured by an MKS type 90 capacitance manometer and controlled by a servoassisted gas-handling system which regulated a Granville-Phillips variable leak.

The initial charge states q of the recoil ions were determined by the time-of-flight (TOF) technique. The time it takes from the production of a recoil ion of mass m to its detection by a channel-electron multiplier (CEM) is proportional to $\sqrt{m/q}$. Typical TOF spectrum for Ne^{q+} ions is shown in Fig. 2.

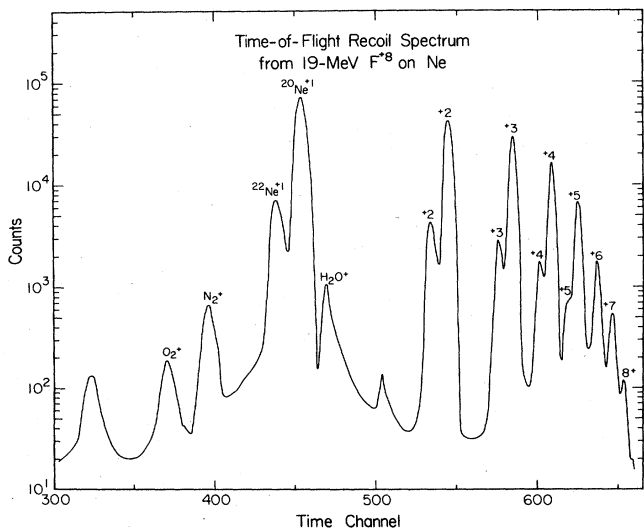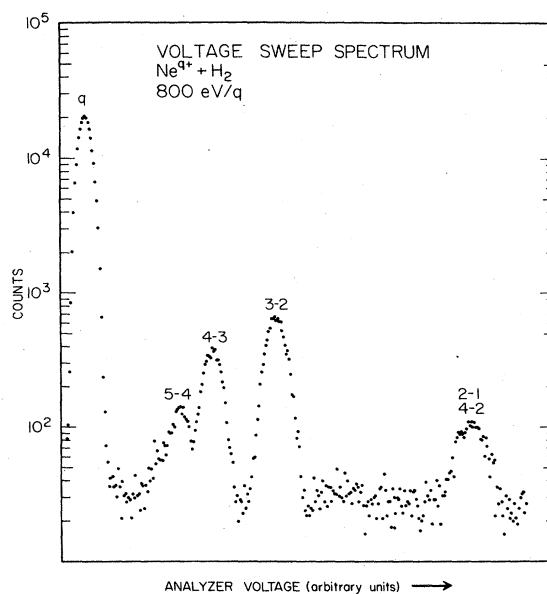The recoil ions were analyzed after their passage through the H_2 gas cell using a double-focusing

spherical-sector electrostatic analyzer. For a given initial energy ($E = qV$) the recoil ion with final charge state q' was detected by the CEM at the analyzing voltage V_a given by

$$V_a = \Gamma \frac{q}{q'} , \qquad (1)$$

where Γ is the product of the accelerating voltage V and the analyzer constant K. The voltage V_a from a programmable power supply was swept repetitively by a triangle wave generator typically in a range from slightly
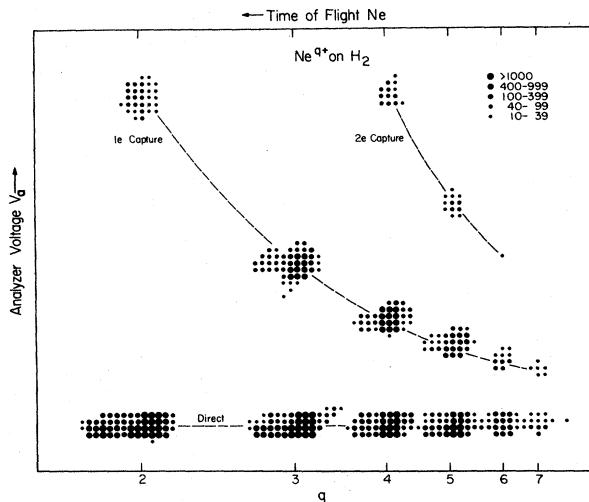

FIG. 2. Typical time-of-flight spectrum for Ne recoils produced by a 19-MeV F^{8+} pump beam. Time of flight increases to the left.

FIG. 4. Two-dimensional coincidence spectrum obtained for Ne^{q+} incident on H_2. Initial recoil-ion charge state is labeled on the abscissa. Single- and double-electron-capture loci are indicated in the figure.

TABLE I. Single-electron-capture cross sections $\sigma_{q,q-1}^{(Ne)}(H_2)$ and $\sigma_{q,q-1}^{(Ar)}(H_2)$ for Ne and Ar on molecular hydrogen in units of 10^{-15} cm^2.

E (eV/q)	$\sigma_{2,1}^{(Ne)}(H_2)$	$\sigma_{3,2}^{(Ne)}(H_2)$	$\sigma_{4,3}^{(Ne)}(H_2)$	$\sigma_{5,4}^{(Ne)}(H_2)$	$\sigma_{6,5}^{(Ne)}(H_2)$	$\sigma_{7,6}^{(Ne)}(H_2)$
200	0.081±0.004	2.33±0.03	3.66±0.07	3.93±0.15	4.49±0.45	
400	0.114±0.005	2.45±0.04	3.21±0.07	3.67±0.16	3.76±0.40	1.86±0.42
600	0.128±0.005	2.64±0.04	3.20±0.07	3.60±0.16	3.70±0.42	
800	0.121±0.005	2.50±0.04	2.87±0.06	3.20±0.013	3.42±0.26	4.04±0.40
1000	0.117±0.005	2.48±0.03	2.98±0.06	2.74±0.12	4.95±0.43	

E (eV/q)	$\sigma_{2,1}^{(Ar)}(H_2)$	$\sigma_{3,2}^{(Ar)}(H_2)$	$\sigma_{4,3}^{(Ar)}(H_2)$	$\sigma_{5,4}^{(Ar)}(H_2)$	$\sigma_{6,5}^{(Ar)}(H_2)$	$\sigma_{7,6}^{(Ar)}(H_2)$	$\sigma_{8,7}^{(Ar)}(H_2)$	$\sigma_{9,8}^{(Ar)}(H_2)$	$\sigma_{10,9}^{(Ar)}(H_2)$
50	0.110±0.006	2.24±0.05	2.93±0.11	2.43±0.12	4.27±0.22	4.10±0.27			
100	0.166±0.009	2.41±0.06	2.86±0.11	3.01±0.15	5.20±0.27	5.50±0.34			
200	0.242±0.007	1.83±0.03	2.87±0.07	2.77±0.11	5.05±0.19	6.17±0.26	4.54±0.25	7.24±0.50	5.40±0.74
520	0.279±0.007	1.62±0.03	2.88±0.07	2.62±0.11	4.20±0.18	5.23±0.25	4.89±0.29	6.53±0.49	3.76±0.62
800	0.244±0.007	1.53±0.03	2.78±0.08	2.82±0.12	5.12±0.20	5.12±0.25	4.59±0.28	4.87±0.41	6.04±0.81
1250	0.266±0.008	1.53±0.03	3.14±0.10	2.92±0.14	4.29±0.21	5.56±0.29	5.25±0.32	7.53±0.55	7.59±0.91
2000	0.282±0.008	1.30±0.03	3.01±0.08	2.61±0.12	4.39±0.20	5.57±0.27	4.81±0.28	5.63±0.46	5.97±0.73
3000	0.258±0.007	1.26±0.03	2.92±0.09	2.71±0.13	4.19±0.21	4.94±0.26	4.74±0.32	5.56±0.49	4.89±0.72

below Γ to above 2Γ (see Fig. 3). For each detected ion the TOF and the analyzer voltage V_a were recorded in list mode by a Digital Equipment Corporation PDP11/34 minicomputer. Using these two parameters a two-dimensional coincidence spectrum (Fig. 4) was obtained for each LEHQ ion energy. These spectra contain the capture and noncapture events.

The absolute cross sections for electron capture were obtained from

$$\sigma_{q,q'} = \frac{N_{q,q'}(x)}{N_q^T(x)x}, \qquad (2)$$

where $N_{q,q'}(x)$ is the yield of an electron-capture event for a given target thickness x, and $N_q^T(x)$ is the total yield (i.e., sum of capture and noncapture events) for a particular initial charge state. The corrections associated with these yields were discussed in detail elsewhere.[13] The absolute value of x was calculated using the known target gas pressure and the gas-cell length. Although throughout these experiments single-collision conditions were maintained, an iterative procedure[15] was used to account for the small contributions due to multiple collisions.

The uncertainties (see Tables I—III) associated with the measured cross sections are based only on statistical considerations. One standard deviation was used as the statistical error for all the relevant yields. A correction for the effective gas-cell length can be made by adding the radii of the cell apertures to the measured length.[16] This would introduce an additional 10% systematic uncertainty to the measured cross sections. This correction was not included in the present measurements.

B. Electron capture from atomic hydrogen

As mentioned before, the basic principles of the measurements of electron capture from either molecular or atomic hydrogen were very similar although the analysis of the data for the atomic-hydrogen target differed greatly from the case of the molecular-hydrogen target. As far as the experimental arrangement was concerned, the main difference was the atomic-hydrogen oven that replaced the second cell used in the measurements for H_2. Therefore, keeping in mind the experimental techniques of Sec. II A, we will now describe the construction and operation of the high-temperature thermal oven that produced the atomic-hydrogen target. The normalization procedure required to obtain absolute cross sections for electron capture by LEHQ ions from atomic hydrogen are also presented in this section.

The oven used in these experiments shared some similarities with those used by other investigators, although its particular application to the recoil-ion technique was tested for the first time in this work. The common feature of hydrogen ovens is the use of a gas cell, a tungsten tube, in which the dissociation of H_2 takes place as a result of catalytic interaction of the gas with the hot surfaces. An alternative way to dissociate molecular hydrogen is to use a dc discharge tube which was first studied by Wood.[17]

A detailed description of the present oven is given elsewhere.[18] Therefore only the essential features of the oven

TABLE II. Double-electron-capture cross sections $\sigma_{q,q-2}^{(Ne)}(H_2)$ and $\sigma_{q,q-2}^{(Ar)}(H_2)$ for Ne and Ar on molecular hydrogen in units of 10^{-15} cm^2.

E (eV/q)	$\sigma_{4,2}^{(Ne)}(H_2)$	$\sigma_{5,3}^{(Ne)}(H_2)$
200	0.084±0.007	0.17±0.03
400	0.069±0.007	0.21±0.04
600	0.097±0.01	
800	0.082±0.08	0.15±0.04
1000	0.069±0.07	

E (eV/q)	$\sigma_{4,2}^{(Ar)}(H_2)$	$\sigma_{5,3}^{(Ar)}(H_2)$	$\sigma_{6,4}^{(Ar)}(H_2)$	$\sigma_{7,5}^{(Ar)}(H_2)$
100	0.59±0.04			
200	0.74±0.03		0.18±0.02	0.17±0.02
520	0.62±0.03	0.71±0.05	0.41±0.05	0.26±0.03
800	0.62±0.03	0.79±0.05	0.36±0.04	0.22±0.03
1250	0.55±0.03			0.22±0.03
2000	0.59±0.03	0.55±0.04	0.29±0.04	0.12±0.02
3000	0.56±0.03		0.31±0.04	0.17±0.03

will be presented in this paper. The heating element of the oven was a 6.4-cm-long and 6-mm-diam tube rolled from 0.025-mm-thick tungsten sheet. Each end of the tube was held between a pair of cylindrical sleeves made of molybdenum, the outer ones being clamped in copper end-plates which in turn were attached to water-cooled electrodes (Fig. 5). The inner cylinders acted as entrance and exit apertures, 1 and 3.5 mm in diameter, respectively. The tube was surrounded by four concentric heat shields made from tantalum. Hydrogen gas was first admitted into the region between the tube and the innermost heat shield, then entered the tube through an ~0.5-mm-wide slit running along the tube. The background measurements were performed by flowing the hydrogen gas directly into the collision chamber whose base pressure was kept below 4×10^{-7} Torr using a 6-in. oil diffusion pump and a 7-in. Varian cryopump. The tube was heated by passing an ~80-A ac current through it and the temperature of the cell (typically 2250 K) was measured by an optical pyrometer through a set of holes drilled radially through the heat shields and aligned with the slit on the tungsten tube. The thermionic electrons emerging from the oven were suppressed by external grids at potentials of −40 V placed near the apertures of the oven. Measurements of ion transmission through the oven did not indicate any measurable effects due to stray magnetic fields on the transmission properties of the LEHQ ions.

The initial and final charge states of the LEHQ ions after their passage through the oven were determined by the experimental techniques discussed in Sec. II A. We normalized our data for the atomic-hydrogen-target measurements to the absolute single-electron-capture cross sections for the molecular-hydrogen target presented in this paper. The normalization technique includes a correction to account for single-electron capture from undissociated H_2 present in the oven. Electron-capture measurements for a fixed input gas flow were carried out running the oven at two different temperatures. The mea-

surements at a low temperature (typically 1350 K) at which there was no dissociation of H_2 provided the yields of electron capture for a molecular-hydrogen target. Similar yields for a mixture of atomic hydrogen and molecular hydrogen were obtained by running the oven at 2250 K. In both cases background measurements were performed with the hydrogen gas flowing directly into the collision chamber.

We now derive a simple expression used for extracting the electron-capture cross sections for interactions with atomic hydrogen. Consider single-electron capture by
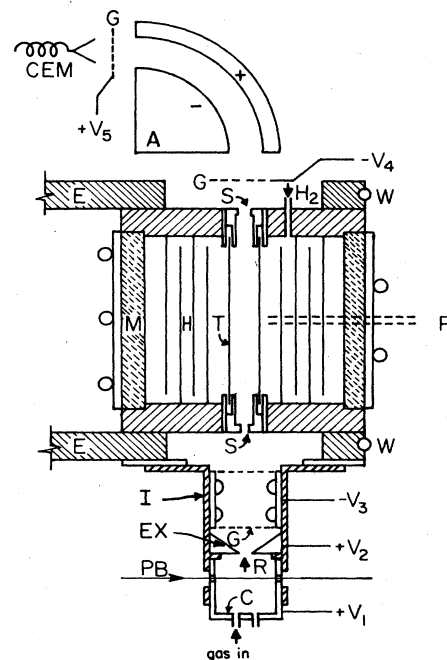

FIG. 5. Hydrogen oven assembly used in this work. Details of the construction of this oven are given in Ref. 18.

TABLE III. Single-electron-capture cross sections $\sigma_{q,q-1}^{(Ne)}(H)$ and $\sigma_{q,q-1}^{(Ar)}(H)$ for Ne and Ar on atomic hydrogen in units of 10^{-15} cm².

E (eV/q)	$\sigma_{2,1}^{(Ne)}(H)$	$\sigma_{3,2}^{(Ne)}(H)$	$\sigma_{4,3}^{(Ne)}(H)$	$\sigma_{5,4}^{(Ne)}(H)$	$\sigma_{6,5}^{(Ne)}(H)$	$\sigma_{7,6}^{(Ne)}(H)$
400	0.045±0.007	1.37±0.12	1.77±0.16	2.70±0.31	1.32±0.36	
600	0.033±0.005	1.55±0.12	1.42±0.14	3.19±0.36	1.27±0.71	
800	0.038±0.017	1.16±0.38	1.29±0.43	2.56±0.65	1.33±0.54	3.15±1.1
1000	0.035±0.006	1.27±0.15	1.49±0.18	2.00±0.22	1.98±0.36	

E (eV/q)	$\sigma_{2,1}^{(Ar)}(H)$	$\sigma_{3,2}^{(Ar)}(H)$	$\sigma_{4,3}^{(Ar)}(H)$	$\sigma_{5,4}^{(Ar)}(H)$	$\sigma_{6,5}^{(Ar)}(H)$	$\sigma_{7,6}^{(Ar)}(H)$	$\sigma_{8,7}^{(Ar)}(H)$	$\sigma_{9,8}^{(Ar)}(H)$	$\sigma_{10,9}^{(Ar)}(H)$
200	0.029±0.014	1.77±0.24	1.92±0.33	2.61±0.40	3.74±0.67	3.83±0.78	2.95±0.68	3.30±1.0	4.48±1.76
520	0.034±0.012	1.48±0.14	1.62±0.20	2.24±0.29	2.90±0.39	2.70±0.41	2.51±0.45	3.63±0.72	1.09±0.48
800	0.044±0.014	1.53±0.16	1.37±0.19	2.37±0.34	2.87±0.48	2.00±0.42	2.48±0.49	2.29±0.56	3.21±1.19
1250	0.052±0.015	1.48±0.26	1.60±0.25	1.84±0.29	2.66±0.43	3.11±0.53	2.52±0.52	4.67±0.97	2.28±1.14

LEHQ ions from molecular hydrogen at a low temperature. Under single-collision conditions, the fraction of LEHQ ions changing their charge state from q to $(q-1)$ is given by

$$N_{q,q-1}(H_2) = \sigma_{q,q-1}(H_2)\pi(H_2) , \qquad (3)$$

where $\pi(H_2)$ is the effective target thickness of H_2. When the gas cell is heated, represented by a superscript asterisk, one obtains a similar expression for single-electron capture from a mixture of atomic and molecular hydrogen:

$$N_{q,q-1}(H,H_2) = \sigma_{q,q-1}(H)\pi^*(H)$$
$$+ \sigma_{q,q-1}(H_2)\pi^*(H_2) , \qquad (4)$$

where $\pi^*(H_2)$ is now smaller than $\pi(H_2)$ of Eq. (3) because of both the increased conductance of the cell at a higher temperature and the dissociation of H_2. Dividing Eq. (4) by Eq. (3) one obtains the normalization expression used in this work:

$$\sigma_{q,q-1}(H) = \sigma_{q,q-1}(H_2)\left[\frac{N_{q,q-1}(H,H_2)}{N_{q,q-1}(H_2)} - \beta\right]\frac{1}{\alpha\beta} , \qquad (5)$$

where $\alpha \equiv \pi^*(H)/\pi^*(H_2)$ and $\beta \equiv \pi^*(H_2)/\pi(H_2)$. Although the electron-capture fractions N^* and N can be easily obtained from the measured yields, the parameters α and β, which represent the performance of the oven under running conditions, need to be determined.

The method most commonly used to determine β requires the measurement of double-electron-capture yields by projectiles incident on H_2 at two different temperatures.[19] The main reason that this method provides reliable results is the fact that, under single-collision conditions, double-electron capture is possible only from molecular hydrogen in the oven.

We have shown in an earlier paper[20] that, under single-collision conditions, the ratio of the fractions of LEHQ ions changing their charge state from q to $(q-2)$ from H_2 at two different operating temperatures determines the value of β, i.e.,

$$\beta = \frac{N^*_{q,q-2}(H,H_2)}{N_{q,q-2}(H_2)} = \frac{\pi^*(H_2)}{\pi(H_2)} . \qquad (6)$$

It was also shown that α and β are related by

$$\sigma = \sqrt{2}\left[\frac{1}{\beta}\left[\frac{T}{T^*}\right]^{1/2} - 1\right] , \qquad (7)$$

where T and T^* denote the low and high oven temperatures, respectively.

In order to determine β we used the yields of double-electron capture for Ne^{4+} and Ar^{4+} recoil ions incident on H_2. The value of β obtained was used along with the measured temperatures to determine α. If a direct measurement of the oven temperature cannot be made one can replace the hydrogen gas by a monoatomic gas such as Ar and perform electron-capture measurements at two operating temperatures as discussed previously.[7] This results in replacing $(T/T^*)^{1/2}$ in Eq. (7) by $N^{*(Ar)}_{q,q-j}/N^{(Ar)}_{q,q-j}$ where j is the number of electrons captured from Ar. All the relevant yields of single- and double-electron capture

by LEHQ ions were obtained with only one set (a total of four runs including background runs) of measurements at each bombarding energy. The typical values of α and β were 2.5 and 0.29, respectively.

The dissociation fraction of H_2 is defined as

$$f \equiv \frac{\pi^*(H)}{\pi^*(H) + 2\pi^*(H_2)}$$

$$= \frac{\alpha}{2+\alpha} = 0.56 \quad \text{for } \alpha = 2.5 . \tag{8}$$

The uncertainties associated with the measured absolute cross sections for electron capture by LEHQ ions from atomic hydrogen were determined using one standard deviation for all the relevant yields and ± 25 K as the error in temperature readings. The error analysis is given in the Appendix. Also given in the Appendix is an analysis of the contributions of double collisions on the measured capture cross sections.

III. RESULTS AND DISCUSSION

A. Molecular-hydrogen target

The dependence of the single- and double-electron-capture cross sections on the initial charge state of incident 1000-eV/q Ne^{q+} and 520-eV/q Ar^{q+} ions are shown in Figs. 6 and 7, respectively, along with the predictions of three theoretical models. The single-electron-capture cross sections for both cases increase with q, although some variations are observed. Such oscillations were also reported for Ar^{q+} ions incident on D_2 by Bli-

man et $al.$[21] and for similar collision systems such as Ne^{q+}+He and Ar^{q+}+He by Cocke et $al.$[9] The classical model[22-25] predicts an oscillatory dependence of the cross sections on the effective charge of the projectile. It is based on the classical transfer of an active electron of a neutral target atom to an incoming ion when the electron has enough energy to overcome the potential barrier between charge centers. This model predicts capture cross sections that are independent of the collision velocity. Electron capture by multiply charged ions in the low-velocity regime has also been calculated in terms of the couplings between the entrance molecular orbital (MO), representing the initially neutral target and charged projectile, and MO's which correlate to an ionized target and projectile.[26] Electron capture may occur through one or more pseudocrossings of the adiabatic energy curves. When a large number of crossings exist around an easily defined internuclear separation an absorbing sphere model[27] may be used to calculate cross sections which exhibit very weakly energy-dependent total capture cross sections. Grozdanov and Janev,[28] using a tunneling model,[29] modified for the inhomogeneous nature of the Coulomb field of the multiply charged ion, observed a linear dependence of the cross sections on the charge of the incident ion. For the absorbing sphere model the q dependence is in good agreement with the general q dependence observed for both Ne^{q+} and Ar^{q+} incident on H_2. The overestimated results of the tunneling model can be attributed to its failure when $q \leq 10$, since the basic assumption of the model that the density of the final states is sufficiently high is not satisfied.

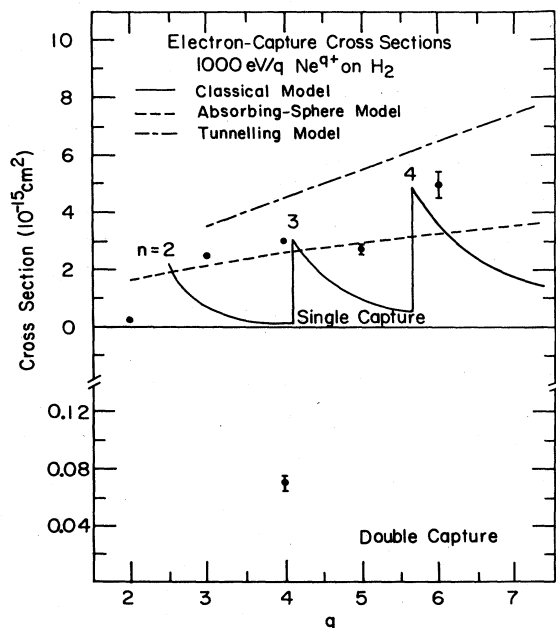The dependences of the single-electron-capture cross

FIG. 6. Charge-state dependence of single- and double-electron capture for Ne^{q+}+H_2 at energies of 1000 eV/q. Numbers embedded within the figure are the principal quantum numbers for the shells into which capture is predicted by the classical model.
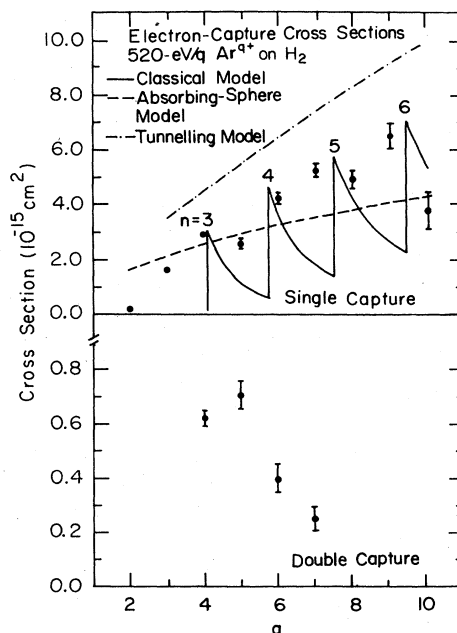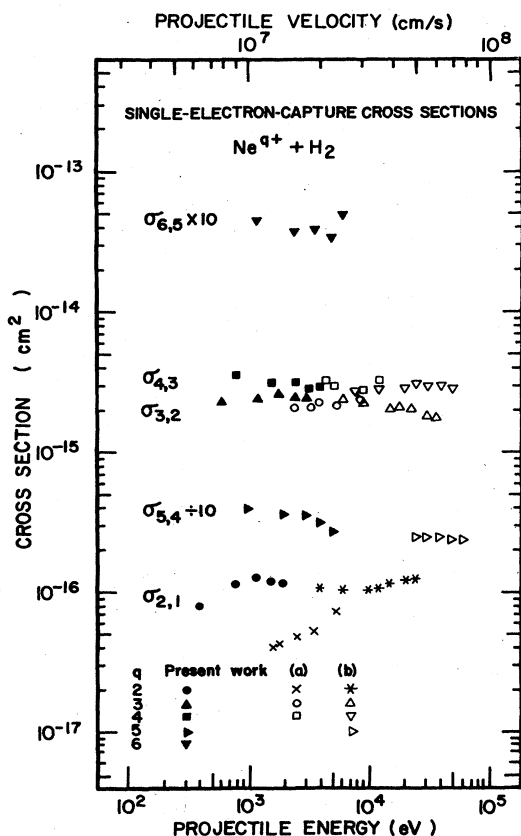

FIG. 7. Charge-state dependence of single- and double-electron capture of Ar^{q+}+H_2 at energies of 520 eV/q. Numbers embedded within the figure are the principal quantum numbers for the shells into which capture is predicted by the classical model.

FIG. 8. Energy dependences of the single-electron-capture cross sections for $Ne^{q+}+H_2$, $q=2-6$. Other results (a) and (b) are from Refs. 5 and 6, respectively.

FIG. 9. Energy dependences of the single-electron-capture cross sections for $Ar^{q+}+H_2$, $q=2-4$ and 7. Other results (a), (b) and (c) are from Refs. 5, 6, and 7, respectively.

FIG. 10. Energy dependences of the single-electron-capture cross sections for $Ar^{q+}+H_2$, $q=5$, 6, 8, and 9. Other results (a), (b) and (c) are from Refs. 5, 7, and 8, respectively.

sections on the energy of the incident Ne^{q+} and Ar^{q+} ions are presented in Figs. 8—10 along with most of the data available in the literature (see Tables I and II for present data). When the results of various measurements covering such a wide energy range (400 eV to ~50 keV for Ne^{q+} and 100 eV to ~600 keV for Ar^{q+}) are examined several observations can be made. First, the cross sections for both Ne^{2+} and Ar^{2+} are small but increase with energy. The present results for both Ne^{2+} and Ar^{2+} incident on H_2 disagree with the measured cross sections by Huber.[5] The reasonably good agreement for higher charge states and the fact that the present results for $q=2$ follow the trend of the measurements at higher energies[6-8] make us believe that the measurements by Huber for $q=2$ may have problems which are not understood at present. It is noted that the results of measurements by Bliman et al.[21] using D_2 targets, not shown in Figs. 9 and 10, are in good agreement for $q\geq3$ but higher for $q=2$ (in an energy range 4—20 keV) by a factor of ~2 than the published data in the same energy range. The cross sections for all other charge states are almost constant over the given energy range including the present results and published data for Ar ions incident on H_2.

The energy dependence and the magnitude of the cross sections can be explained in terms of the couplings between the MO's correlating to the entrance and the exit
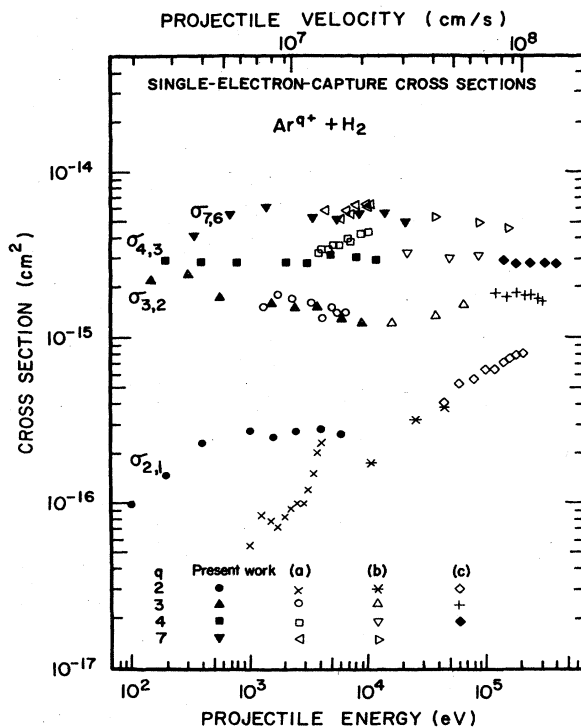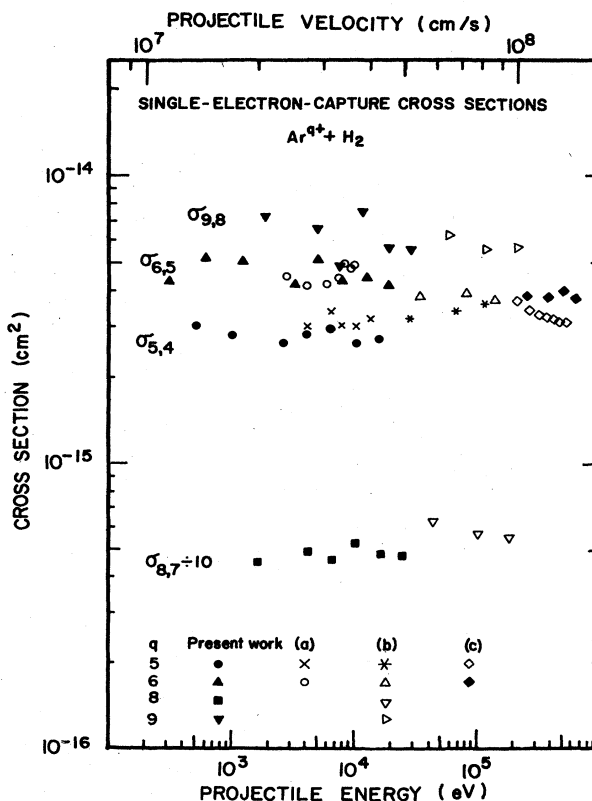
channels. The exit channel MO's undergo long-range crossings with those of the entrance channel due to the strong repulsive Coulomb potential of the product ions, provided they correspond to an exoergic reaction. The energy-independent cross sections for $q \geq 3$ are due to the availability of many exoergic channels so that any dependence on energy for a particular exit channel is washed out in the sum over many other reactions. On the other hand, the relatively few number of exoergic channels for $q = 2$ not only results in small cross sections, but also indicates dependence on energy when one of these channels contributes strongly to the cross sections. The electron-capture cross sections can be estimated using the energy defects ΔE for the process. If the polarization effects are ignored, the pseudocrossing for exoergic reactions occur at internuclear separation, $R_c \approx q - 1/\Delta E$ (a.u.). The cross sections are calculated using $\sigma = \pi R_c^2$. As an example consider the single-electron capture by Ne^{2+} incident on H_2. There is only one excited final state of Ne^{1+} for which the capture reaction is exoergic with $\Delta E \approx 26$ eV, calculated using the atomic energy level tables of Moore.[30] The crossing occurs at $R_c \approx 1$ a.u. and the cross section ($\sim 10^{-16}$ cm^2) agrees with the measured value quite well. This is also true for Ar^{2+} projectiles, and the crossing radius, $R_c \approx 2.3$ a.u., corresponding to $\Delta E \approx 12$ eV, yields a reasonable estimate for the cross section. When the higher initial charge states such as Ar^{3+} and Ne^{3+} are considered, one observes that the number of exoergic channels increases, which results in a wide range of energy defects and corresponding contributions to the cross sections. For example, for $Ar^{3+} + H_2$, the final state of the projectile is expected to be $Ar^{2+} (1s^2 2s^2 2p^6 3s\, 3p^5)$. The energy defect for this particular reaction ($\Delta E \approx 11$ eV) is consistent with the measured[31] value ($\Delta E \approx 15 \pm 4$ eV). The cross section obtained in this way using $R_c \approx 5$ a.u. agrees with the measured data. Furthermore, the absorbing sphere model predicts a crossing around 5 a.u. and the classical model calculation predicts the capture to proceed to $n = 3$ with $R_c \approx 6$ a.u. Similar arguments can also be made for other collision systems.

B. Atomic-hydrogen target

The dependence of the electron-capture cross sections on the initial charge state of Ne^{q+} and Ar^{q+} incident on H is shown in Fig. 11 together with the predictions of model calculations. Once again, variations with the incident charge state are observed in the measured cross sections. The predictions of the classical model seem to follow the trend of the data, but significant differences are observed when the present data are compared with the predictions of the absorbing sphere model or the tunneling model,[32] both calculated at a collision velocity of 7×10^7 cm/s. However, it should be pointed out that the predictions of the absorbing sphere model are expected to provide reasonable agreement only for the very high charge states. This is because of the fact that for high q a high density of curve crossing may be found at large internuclear distances. On the other hand, for lower q the cross sections depend strongly on the molecular structure of the colliding pair since a high density of curve crossings is not
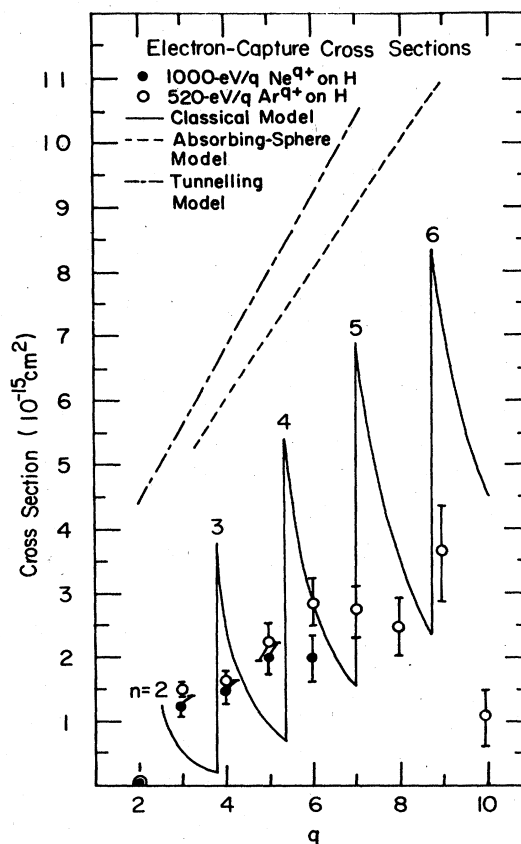

FIG. 11. Charge-state dependences of Ne^{q+} and Ar^{q+} incident upon H at energies of 1000 and 520 eV/q, respectively.
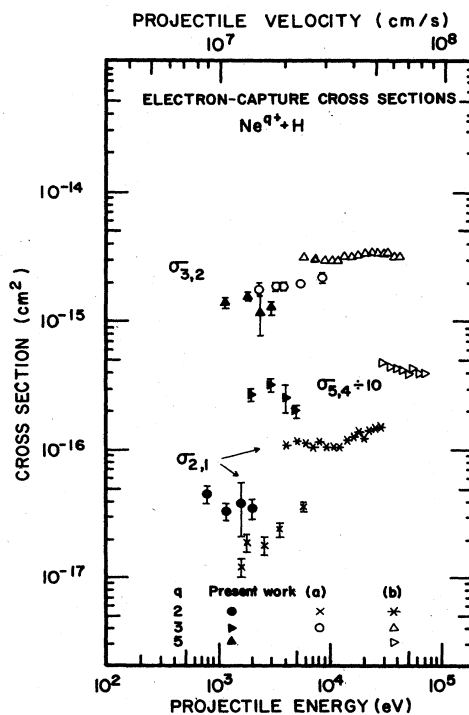

FIG. 12. Energy dependences of the electron-capture cross sections for $Ne^{q+} + H_2$, $q = 2$, 3, and 5. Other results (a) and (b) are from Refs. 5 and 6, respectively.
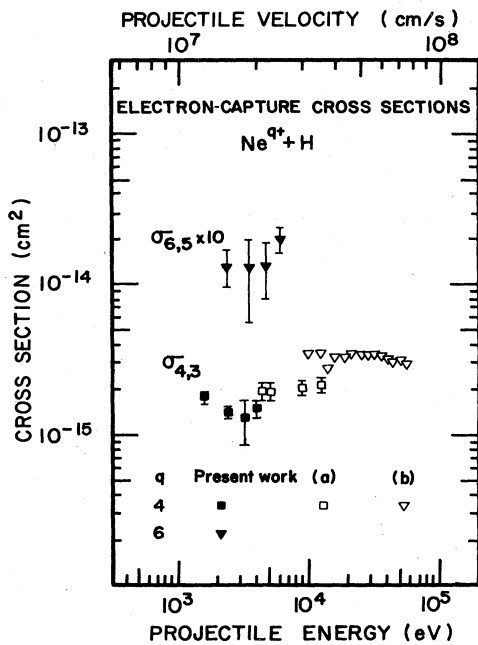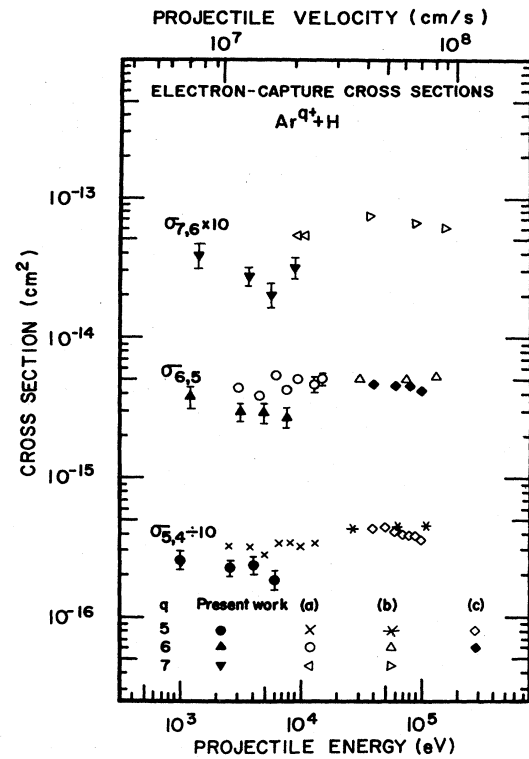
FIG. 13. Energy dependences of the electron-capture cross sections for $Ne^{q+}+H_2$, $q=4$, and 6. Other results (a) and (b) are from Refs. 5 and 6, respectively.
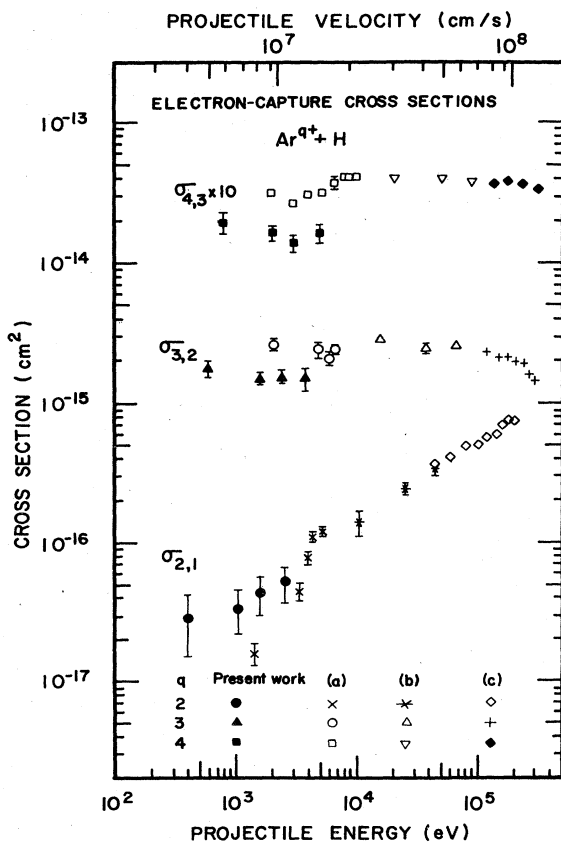

FIG. 14. Energy dependences of the electron-capture cross sections for $Ar^{q+}+H_2$, $q=2-4$. Other results (a), (b) and (c) are from Refs. 5, 7, and 8, respectively.

FIG. 15. Energy dependences of the electron-capture cross sections for $Ar^{q+}+H_2$, $q=5-7$. Other results (a), (b) and (c) are from Refs. 5, 7, and 8, respectively.

available. The overestimated results of the tunneling model[32] can also be understood in terms of the lack of a high density of final states for $q \leq 10$.

The energy dependence of the cross sections for Ne^{q+} and Ar^{q+} incident on H is shown in Figs. 12 and 13 and Figs. 14 and 15, respectively (see also Table III). Also shown in these figures are the measured cross sections available from the literature.[5-7] In the case of $Ne^{q+}+H$ the present data agree reasonably well with those of Huber[5] provided his data for $q=2$ are normalized to the present results for $Ne^{2+}+H_2$. But the cross sections for atomic hydrogen reported by Seim et al.[6] do not agree with neither set of measurements, although there exists good agreement among the various measured data for H_2. The present results and those of Huber[5] indicate that the ratio $\sigma_{q,q-1}(H)/\sigma_{q,q-1}(H_2)$ for Ne^{q+} is always smaller than 1, whereas Seim et al.[6] obtained values ≥ 1.

When the results of various measurements for $Ar^{q+}+H$ are compared a similar picture emerges. The cross sections for $Ar^{2+}+H$ increase with energy and the present results agree with the trend of the published[5-7] and unpublished[8] results at higher energies quite well, provided the measurements by Huber[5] are normalized to the results of the present work on H_2. In the case of higher charge states, the agreement between the present work and the results from the sources mentioned above is fair. The reasons for differences are not understood at present.

The relatively small and energy-dependent cross sec-

tions for Ne^{2+} and Ar^{2+} incident on H can be explained in terms of energy defects for the capture reactions that are exoergic. For example, for the collision system $Ne^{2+}+H$, there is only one final state $(1s^2 2s^2 2p^5\, {}^2P)$ with reasonably exoergicity $(\Delta E \approx 27.5$ eV) corresponding to a crossing at $R_c \sim 1$ a.u. and the estimated cross section $(9 \times 10^{-17}$ cm$^2)$ is a factor of 2 higher than the present results. Similar arguments indicate that for $Ar^{2+}+H$, the only reasonable exoergic channel is a capture to the $3p$ subshell of the incoming ion with $\Delta E \approx 14$ eV and $R_c \approx 2$ a.u. The cross section calculated in this manner $(3.4 \times 10^{-16}$ cm$^2)$ is larger than the measured cross section.

In summary, we have measured cross sections for electron capture by LEHQ Ne^{q+} and Ar^{q+} ions incident on H_2 and H in a velocity regime somewhat lower than those previously investigated. Absolute cross sections for electron capture were measured for both collision systems. In the case of measurements on H_2, there is generally good agreement between the present results and the results available from different sources. But there exist some differences between various measurements for H for which the reasons are not understood.

In order to gain insight into the collision dynamics of the electron-capture process by LEHQ projectiles from one- or many-electron targets, new experiments, more selective in nature, are being carried out at different laboratories. It is now possible to determine the principal quantum number n of the projectile electron shell which is populated by the electron capture from spectroscopic analysis[22-25] or from a study of the final kinetic energy distribution,[32-34] of the projectile after the collision. Experimental studies of the energy gain spectroscopy for collision systems like $Ne^{q+}+H$ and $Ar^{q+}+H$ should provide interesting information on the contribution of relevant n values of the capture process to test the predictions of new theoretical models.

ACKNOWLEDGMENTS

APPENDIX

So far we have excluded the second-order terms, representing the double-collision effects, i.e., sequential interactions from separate atoms and/or molecules, in all the derivation particularly for α and β. Now we discuss and justify the reasons for ignoring such corrections. As an example, consider the case of 800-eV/q Ar^{4+} incident on the molecular- and atomic-hydrogen targets at running temperatures, $T = 1423$ K and $T^* = 2273$ K, respectively. Using the measured data and the cross section for single-electron capture from H_2 one obtains from Eq. (2),

$$\pi(H_2) = \frac{N_{4,3}(H_2)}{N_4^T \sigma_{4,3}(H_2)}$$

$$= 7.75 \times 10^{12} \text{ molecules/cm}^2 . \tag{A1}$$

On the other hand, calculating the target density gives

$$\pi(H_2) = \frac{N_A}{2.24 \times 10^4} \frac{P(\text{mTorr})}{7.6 \times 10^5 \text{ mTorr}} \frac{273 \text{ K}}{1423 \text{ K}} 7.5 \text{ cm}$$

$$= 5.1 \times 10^{13} P(\text{mTorr}) \text{ molecules/cm}^2 \text{mTorr} , \tag{A2}$$

where N_A is Avogadro's number and P is the pressure in mTorr. The pressure of H_2 gas in the oven at $T = 1423$ K is found to be 0.15 mTorr.

The effects of double collisions on the electron-capture yields will be important especially in the case of two-electron-capture measurements. Therefore we now consider Eq. (4) for the particular case of incident Ar^{4+} ions, including second-order scattering corrections,

$$N_{4,2}(H_2) = \sigma_{4,2}(H_2)\pi(H_2)$$
$$+ \sigma_{4,3}(H_2)\sigma_{3,2}(H_2)[\pi(H_2)]^2 . \tag{A3}$$

Using the measured cross sections, presented in Table I, and $\pi(H_2)$ determined above, one obtains

$$N_{4,2}(H_2) = (0.62 \times 10^{-15})(7.75 \times 10^{12})$$

$$+ (2.78 \times 10^{-15})(1.53 \times 10^{-15})(7.75 \times 10^{12})^2$$

$$= 4.81 \times 10^{-3} + 2.55 \times 10^{-4} . \tag{A4}$$

We see that the second-order term on the right-hand side is about 5% of the single-collision term. Therefore one can ignore the effects of double collisions for the measurements using H_2 targets.

Similarly, for the high-temperature (hot oven) measurements the fractional yield for $N_{4,2}^*(H,H_2)$, including second-order scattering corrections, is given by

$$N_{4,2}^*(H,H_2) = \sigma_{4,2}(H_2)\pi^*(H_2) + \sigma_{4,3}(H_2)\sigma_{3,2}(H_2)[\pi^*(H_2)]^2 + \sigma_{4,3}(H)\sigma_{3,2}(H)[\pi^*(H)]^2$$
$$+ [\sigma_{4,3}(H)\sigma_{3,2}(H_2) + \sigma_{4,3}(H_2)\sigma_{3,2}(H)][\pi^*(H)\pi^*(H_2)] . \tag{A5}$$

Using $\alpha = \pi^*(H)/\pi^*(H_2) = 2.50$ and $\beta = \pi^*(H_2)/\pi(H_2) = 0.29$ we find that

$$N_{4,2}^*(H,H_2) = 1.39 \times 10^{-3} + (2.15 \times 10^{-5} + 6.53 \times 10^{-5}$$

$$+ 7.96 \times 10^{-5}) , \tag{A6}$$

and the sum of the second-order terms (in parentheses) is only 12% of the first-order term.

If the contributions due to double collisions are subtracted from the measured $N_{4,2}^*(H,H_2)$ and $N_{4,2}(H_2)$ we obtain $\beta = 0.27$ and $\alpha = 2.78$ whereas without such corrections we had obtained $\beta = 0.29$ and $\alpha = 2.50$. Using the corrected values of α and β one calculates the cross section, for example, $\sigma_{4,3}(H) = 1.31 \times 10^{-15}$ cm^2 which is the same as before. Note that the cross section given in Table III $[\sigma_{4,3}(H) = 1.37 \times 10^{-15}$ cm$^2]$ is the average value ob-

tained from three separate measurements. Therefore, such effects are indeed considered small, since they do not change the values of α and β significantly.

The following expressions were used to determine the relative uncertainties associated with various measured quantities involved in the experiments using the atomic-hydrogen target.

(i) Using $f = \alpha/(2+\alpha)$ one obtains the relative uncertainty in the measured dissociation fraction as

$$\frac{\Delta f}{f} = \frac{2\,\Delta\alpha}{\alpha(2+\alpha)} \, , \tag{A7}$$

where

$$\Delta\alpha = \left\{ (\alpha+\sqrt{2})^2 \left[\left[\frac{\Delta N_{q,q-2}(H_2)}{N_{q,q-2}(H_2)} \right]^2 + \left[\frac{\Delta N^*_{q,q-2}(H,H_2)}{N^*_{q,q-2}(H,H_2)} \right]^2 + \left[\frac{\Delta T}{2T} \right]^2 + \left[\frac{\Delta T^*}{2T^*} \right]^2 \right] \right\}^{1/2} . \tag{A8}$$

(ii) Since α and β are independent Eq. (5) can be rewritten using Eq. (7) as

$$\sigma_{q,q-1}(H) = \frac{\sigma_{q,q-1}(H_2)}{\sqrt{2}} \left[\frac{N^*_{q,q-1}(H,H_2)/N_{q,q-1}(H_2)-\beta}{(T/T^*)^{1/2}-\beta} \right] . \tag{A9}$$

One obtains the relative uncertainty in the measured cross sections for the atomic-hydrogen target as

$$\frac{\Delta\sigma_{q,q-1}(H)}{\sigma_{q,q-1}(H)} = \left\{ \left[\frac{\Delta\sigma_{q,q-1}(H_2)}{\sigma_{q,q-1}(H_2)} \right]^2 + \left[\frac{1}{1-\beta[N_{q,q-1}(H_2)/N^*_{q,q-1}(H,H_2)]} \right]^2 \right.$$

$$\times \left[\left[\frac{\Delta N^*_{q,q-1}(H,H_2)}{N^*_{q,q-1}(H,H_2)} \right]^2 + \left[\frac{\Delta N_{q,q-1}(H_2)}{N_{q,q-1}(H_2)} \right]^2 \right]$$

$$+ \frac{1}{4} \left[\frac{1}{1-\beta(T^*/T)^{1/2}} \right]^2 \left[\left[\frac{\Delta T}{T} \right]^2 + \left[\frac{\Delta T^*}{T^*} \right]^2 \right] + \left[\frac{\beta}{N^*_{q,q-1}(H,H_2)/N_{q,q-1}(H_2)-\beta} + \frac{\beta}{(T/T^*)^{1/2}-\beta} \right]^2$$

$$\times \left[\left[\frac{\Delta N^*_{q,q-1}(H,H_2)}{N^*_{q,q-2}(H,H_2)} \right]^2 + \left[\frac{\Delta N_{q,q-2}(H_2)}{N_{q,q-2}(H_2)} \right]^2 \right] \right\}^{1/2} . \tag{A10}$$

In calculating the relative uncertainties for the measured cross sections one standard deviation was used as the uncertainty in single- and double-electron-capture yields. The uncertainty in the measured values of the temperatures was ± 25 K.

*Permanent address: Department of Physics, University of South Alabama, Mobile, AL 36688.

[1]C. M. Meade, Nucl. Fusion 14, 289 (1974).

[2]J. Hogan and H. C. Howe, Bull. Am. Phys. Soc. 20, 1228 (1975).

[3]H. B. Gilbody, Phys. Scr. 23, 143 (1981).

[4]R. A. Phaneuf, Phys. Rev. A 24, 1138 (1981).

[5]B. A. Huber, Z. Phys. A 299, 307 (1981). See also Ref. 32 for $Ar^{q+} + H_2$ data.

[6]W. Seim. A. Müller, I. Wirkner-Brott, and E. Salzborn, J. Phys. B 14, 3475 (1981). The data for $Ne^{q+} + H_2$ were taken from W. Seim, Ph.D. Dissertation, Justus-Liebig-Universität, Giessen (1981).

[7]D. H. Crandall, R. A. Phaneuf, and F. W. Meyer, Phys. Rev. A 22, 379 (1980).

[8]T. V. Goffee (private communication).

[9]C. L. Cocke, R. DuBois, T. J. Gray, and E. Justiniano, IEEE

Trans. Nucl. Sci. NS-28, 1032 (1981).

[10]C. L. Cocke, Phys. Rev. A 20, 749 (1979).

[11]T. J. Gray, C. L. Cocke, and E. Justiniano, Phys. Rev. A 22, 849 (1980).

[12]I. A. Sellin, C. R. Vane, S. B. Ellston, J. P. Forester, P. M. Griffin, D. J. Pegg, R. S. Thoe, K.-O. Groenweld, R. Laubert, and F. Chen, Z. Phys. A 283, 329 (1977).

[13]E. Justiniano, C. L. Cocke, T. J. Gray, R. D. DuBois, and C. Can, Phys. Rev. A 24, 2953 (1981).

[14]E. Justiniano, Ph.D. dissertation, Kansas State University, 1981 (unpublished).

[15]S. K. Allison, Rev. Mod. Phys. 30, 1137 (1958).

[16]D. H. Crandall, M. L. Mallory, and D. C. Kocher, Phys. Rev. A 15, 61 (1977).

[17]R. W. Wood, Proc. R. Soc. London. Ser. A 97, 455 (1920).

[18]C. Can, T. J. Gray, J. M. Hall, L. N. Tunnell, and S. L. Varghese, IEEE Trans. Nucl. Sci. NS-30, 943 (1983).

[19]G. J. Lockwood, H. F. Helbig, and E. Everhart, J. Chem. Phys. **41**, 3820 (1964).

[20]T. J. Gray, C. Can, J. M. Hall, L. N. Tunnell, and S. L. Varghese, IEEE Trans. Nucl. Sci. **NS-30**, 895 (1983).

[21]S. Bliman, J. Aubert, R. Geller, B. Jacquot, and D. van Houtte, Phys. Rev. A **23**, 1703 (1981).

[22]R. Mann, F. Folkmann, and H. F. Beyer, J. Phys. B **14**, 1161 (1981).

[23]R. Mann, H. F. Beyer, and F. Folkmann, Phys. Rev. Lett. **46**, 646 (1981).

[24]H. F. Beyer, K.-H. Schartner, and F. Folkmann, J. Phys. B **13**, 2459 (1980).

[25]H. Ryufuku, K. Sasaki, and T. Watanabe, Phys. Rev. A **21**, 745 (1980).

[26]R. E. Olson, in *Invited Papers and Progress Reports of the XI International Conference on the Physics of Electronic and Atomic Collisions, Kyoto, 1979,* edited by N. Oda and K. Takayanagi (North-Holland, Amsterdam, 1980), p. 391.

[27]R. E. Olson and A. Salop, Phys. Rev. A **14**, 579 (1976).

[28]T. P. Grozdanov and R. K. Janev, J. Phys. B **13**, L69 (1980).

[29]M. I. Chibisov, Pis'ma Zh. Eksp. Teor. Fiz. **24**, 67 (1976) [JETP Lett. **24**, 56 (1976)].

[30]C. E. Moore, *Atomic Energy Levels,* Natl. Bur. Stand. (U.S.) Circular No. 467 (U.S. GPO, Washington, D.C., 1971).

[31]B. A. Huber and H. J. Kahlert, J. Phys. B **13**, L159 (1980).

[32]T. P. Grozdanov and R. K. Janev, Phys. Rev. A **17**, 880 (1978).

[33]R. Mann, C. L. Cocke, A. S. Schlachter, M. Prior, and R. Marrus, Phys. Rev. Lett. **49**, 1329 (1982).

[34]H. J. Kahlert, B. A. Huber, and K. Wiesmann, J. Phys. B **16**, 449 (1983).